Chapter 5

Accelerator Design

5.1 Accelerator Overview

New science and scientific schemes proposed and discussed in the previous chapters would greatly benefit from an upgrade of the light source. One of the examples is that significant increase in light brilliance may open an opportunity to implement new observations of inhomogeneous objects via statistical analyses. Another example is a coherent diffraction imaging that relies on transverse coherent characteristic of the light. For the purpose, the SPring-8 upgrade plan aims at significant improvement in light source qualities, especially in brilliance and coherence [1,2]. The keyword is the diffraction limit in the X-ray region. The quality of radiation, either synchrotron radiation emitted from a bending magnet or undulator radiation from an insertion device, depend on that of the source, which in our case is electron bunches. The quality of electron bunches can be measured by so-called emittance, of which definition is a product of a bunch size and a divergence angle. If the electron emittance were negligibly small, the quality of radiation would be dominated by the intrinsic product of radiation size and its divergence. The intrinsic product is referred as a diffraction limit, known to be $\lambda/4\pi$, where λ is the wavelength of the light. For the existing SPring-8, however, the emittance of electron beams stored in a storage ring has exceeded the diffraction limit of light by orders of magnitudes, thereby the quality of light is dominated by the electron emittance, which is most likely the case for other storage rings as well.

As the electron emittance approaches the diffraction limit of the light, the spatial coherent fraction approaches the unity, and the brilliance comes close to the maximum given by so-called zero-emittance beam. The goal of the SPring-8 upgrade plan is to achieve the electron emittance that is equivalent to the diffraction limit of light in the X-ray region. Such a goal has been regarded as "ultimate" in storage rings, originally coined by Ropert [3]. Note that the diffraction limit, $\lambda/4\pi$, is proportional to the wavelength of light, or inversely proportional to the photon energy. So the diffraction limit becomes smaller as the electron energy becomes

higher to generate higher photon energies. Moreover, the equilibrium emittance in a storage ring is proportional to the square of the electron energy (see Eq.(5.1)); lower energy electrons intrinsically yield better emittance for a given lattice. In consequence, one finds it more difficult to achieve the diffraction limited ring for higher electron/photon energies, although it is extremely important to challenge the future scientific opportunities in the hard X-ray region.

In this chapter, major requirements and constraints for upgrading the SPring-8 accelerator complex, and the basic concept and approach for meeting the user demands are described. Important details of individual accelerator components and the related physics are presented in a separate report [1].

5.1.1 Scope of SPring-8 II Accelerator Complex

Figure 5.1 shows the current view of the SPring-8 site. On the site, there are two main accelerators; a storage ring called SPring-8 (top right in Fig.5.1) , and a linac-based XFEL called SACLA (left). The current SPring-8 accelerator complex is composed of a 1 GeV linear accelerator (linac), a 8 GeV booster synchrotron, and a 8 GeV storage ring. The upgrade plan mainly focuses on modifying the whole part of the storage ring including insertion devices and beamlines. As an injector, we plan to make use of the XFEL linac that generates an unnormalized emittance of tens of pm.rad.

The newly designed storage ring features a multi-bend lattice with damping wigglers, which allows us to reduce natural emittance by two orders of magnitudes or more compared with the current SPring-8 double-bend lattice without damping wigglers. The final natural emittance will reach or come close to the diffraction limit of light in the X-ray region. In order to realize the goal, new technology developments will be indispensable and is discussed in the report. Note that some detailed verifications of the technology developments are still open at the moment, and the R&D are underway. In the following sections, we shall begin with a new lattice design that is expected to bring the emittance down to the regime of diffraction limit. The technologies that support the lattice design are then briefly overviewed in the report. Some of more detailed discussion on the technologies are found in Ref. [1].

5.1.2 Basic Constraints and Design Criteria

At the SPring-8 upgrade, the new storage ring will not be built in a new building, but is planned to replace the existing accelerator system. Therefore the new storage ring lattice has to fit in the existing SPring-8 tunnel. The constraints for the upgrade plan are summarized in the following.

Considering cost-effectiveness and influences on current and future users, the following constraints are set in the SPring-8 upgrade design:

1) The new storage ring will be built in the existing tunnel.

Figure 5.1: SPring-8 Accelerator Complex; SPring-8 (right top) and SACLA (left).

2) Existing insertion device beamlines should stay in existing hutches.

3) Shutdown time should be about a year.

In addition to the three major constraints, it is required that the new ring should provide an adequate beam stability for user experiments. Although the brilliance and the coherence of light may be the first figure of merit for the new design, we regard the stability as equally important criterion as the light qualities. Since the beam dynamics in a storage ring tends to be less stable as a newly designed lattice approaches the diffraction limit in terms of beam dynamics and technological challenges, it is an important strategy in a design to find a good compromise between the light quality and the stability.

A top-up operation is as well one of key features for recent storage rings. SPring-8 has provided the top-up operation since 2004 so that the heat loads are kept stable and the constant flux of light are provided to beamlines. A flexibility of the filling pattern is also an important feature. The flexibility will be determined by wakefield calculations and a beam loading effect in cavities. The bottom line is that the advantages of the current SPring-8 should be maintained, while the accelerator performances are significantly upgraded. The currently available features are already taken for granted.

Nowadays to built an energy-efficient and environmentally friendly facility is a crucial matter to accommodate with a sustainable society. In the design of a new storage ring at the SPring-8 site, we shall strive to construct an energy-concious accelerator facility, still meeting high demands for future sciences.

5.1.3 Design Goals for the Upgraded Accelerator

The SPring-8 upgrade plan sets an ultimate goal that the new storage ring would provide extremely high quality electron beams of which emittance reaches the diffraction limit of light in the X-ray region. The diffraction limit corresponds to 10 pm.rad for 10 keV photons, for example. When the electron beam quality reaches the level, the brilliance is almost saturated as presented in Fig. 5.2 and the coherent fraction gets close to unity. In Fig. 5.2, the brilliance is calculated at the photon energy of 10 keV under conditions that the electron energy is 6 GeV, the current 100 mA, coupling ratio 0.02, energy spread 0.12 %, and betatron functions 1.0 meter in both horizontal and vertical axes as an example. As one can see, the brilliance effectively increases as the electron emittence decreases from a few nm.rad to tens of pm.rad. Although there would still be gain in the brilliance and the coherent fraction beyond the diffraction limit until the electron emittance reaches zero, the effectiveness would become smaller while the difficulty and costs would become much higher. Therefore, the diffraction limit is set as a *reasonable* ultimate goal for the SPring-8 upgrade.

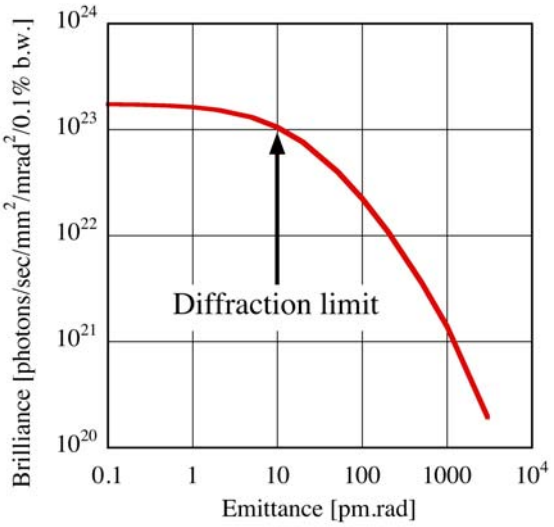

Figure 5.2: Brilliance vs Emittance. Brilliance is estimated at 10 keV, of which diffraction limit corresponds to 10 pm.rad. Electron energy of 6 GeV, current of 100 mA, coupling ratio of 0.01, energy spread of 0.12 %, and betatron functions of 1.0 meter in horizontal and vertical axes are assumed.

A short X-ray pulse generation is also an option of the upgrade. In general, storage rings have been regarded as high average brilliance/flux light sources, while linac based light sources such as XFELs and ERLs are likely expected to provide high peak brilliance/flux. The reason is that a natural bunch length, i.e., an equilibrium bunch length determined by stochastic nature of beam dynamics in a storage ring, is normally longer than that can be generated by linear accelerators. Furthermore, it is often required that the bunch duration should be lengthened by external devices in order to suppress the intra-beam scattering effect; otherwise low emittance

of stored bunches are deteriorated by mutual collisions between electrons. We have considered a possibility of generating short X-ray pulses without affecting the extremely low emittance, since the short time scale in a range of subpico- to pico-second is of great importance especially when pump-and-probe experiments are demonstrated (see Chapter 4).

In the present chapter, the conceptual design of the accelerator system as well as critical issues for materializing the design are presented. The resulting performance of the design as a light source is summarized in Chapter 6.

5.2 Conceptual Design of the Accelerator

5.2.1 Storage Ring Lattice

The goal of the upgrade plan is to realize a "diffraction limited" hard X-ray source and an ultimate target value of the emittance is set to be 10 pm.rad, about 1/300 of the current value. Such a small emittance cannot be realized by the present storage ring lattice of the double-bend type and hence its drastic modification is inevitable.

The equilibrium horizontal emittance, ϵ, is written as,

$$\epsilon = C\frac{E^2}{N^3}, \tag{5.1}$$

where C is a constant determined by a lattice, E is an electron energy, and N is the number of bending magnets (see, for example, [4, 5] for detailed definition). The constant C can be minimized by employing the theoretical minimum emittance (TME) lattice [4]. However, to decrease the constant C is not enough for approaching extremely small emittance. Thus, we plan to modify both the electron energy E and the number of bending magnets N.

We carried out feasibility studies of converting the lattice from the double-bend type, i.e. $N = 2$, to a multi-bend type, $N > 2$, having the arc structure close to the TME [3, 6–11]. Due to the constraint that the ring circumference is fixed and the number and positions of straight sections for insertion devices are unchanged, the new lattices have to keep roughly the same cell length and the existence of four long straight sections. Starting from the double-bend lattice we increased the number of bending magnets in a unit cell one by one and checked linear and nonlinear beam dynamics issues [12–14].

All the newly designed lattices assume the electron energy of 6 GeV. The decrease of the energy from 8 GeV should give an emittance reduction by a factor of ~2 according to Eq.(5.1). In addition, the lower energy helps relax required magnet strengths, allow a higher beam current, make an energy spread narrower, and maximize damping wiggler effects, although the harmful effects of intrabeam scattering and shortening of Touschek beam lifetime must also be considered. The decrease of the electron energy relies on developments of insertion devices. Shorter

period undulators have made it possible to generate higher photon energies for a given electron energy, which has supported recent projects of new light sources. Even further advances will be expected in the future. At present, we choose the beam energy of 6 GeV as a most possible candidate for the challenging goal, and in what follows beam parameters are calculated at this energy. More detailed discussion on the choice of electron energy will be presented in Section 5.4 and Ref. [1].

Unit Cell

Figure 5.3 shows the present double-bend lattice of the SPring-8 storage ring. The natural emittance is ϵ = 3.4 nm.rad at 8 GeV, while the effective one at the normal straight section (with dispersion leakage) is $\epsilon_{\rm eff}$ = 3.7 nm.rad. When we lower the beam energy from 8 to 6 GeV and impose the achromat condition, the emittance becomes about ϵ = 4 nm.rad.

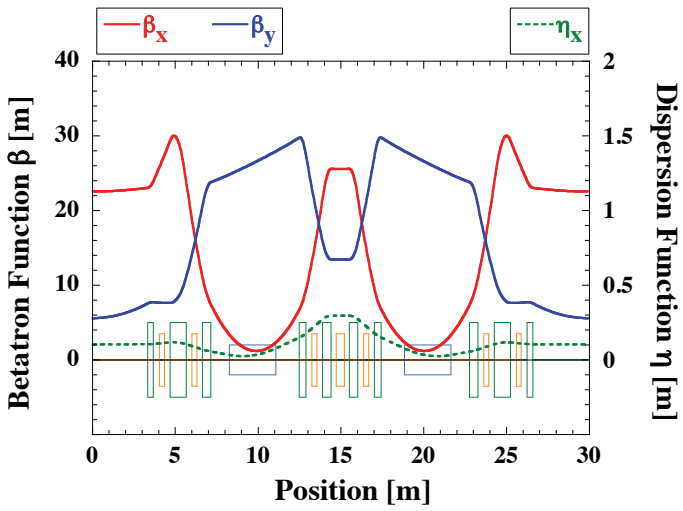

Figure 5.3: The present double-bend lattice of the SPring-8 storage ring. The lattice functions and magnet arrangement (blue: bending, green: quadrupole, orange: sextupole) are shown for a unit cell.

By changing the lattice structure to multi-bend type and increasing the number of bending magnets N, we can reduce the emittance as shown in Fig. 5.4. This procedure of emittance reduction has, however, a practical limit at some value of N, since the cell length is fixed and as we require a smaller emittance the focal length of quadrupole magnets becomes shorter and hence their strengths become stronger, yielding large natural chromaticities. Then, strong sextupole magnets are required and the dynamic aperture shrinks. For example, the horizontal dynamic aperture calculated at β_x = 20 m with 10 μm (rms) alignment errors of sextupole magnets is about ±15 mm for N = 2, and it shrinks to ±10 mm for N = 3 and to ±2 mm for N = 6. By considering the achievable emittance, required magnet strengths and the resulting dynamic aperture, we have currently chosen a 6 bend lattice (N = 6) as the most promising

candidate for an upgraded storage ring lattice. Figure 5.5 shows the lattice functions of the 6 bend achromat optics. The betatron functions at normal straight sections are about 1 m in both horizontal and vertical directions. This is for maximizing the brilliance of synchrotron radiation and for allowing a small minimum gap of insertion devices. In Fig. 5.5 we also show the arrangement of bending, quadrupole and sextupole magnets. The design of quadrupole and sextupole magnets must be as compact as possible, having an optimized pole shape and capability of generating high field gradient. The interference of reciprocal magnetic fields must be considered and a suitable design of the vacuum chamber is needed.

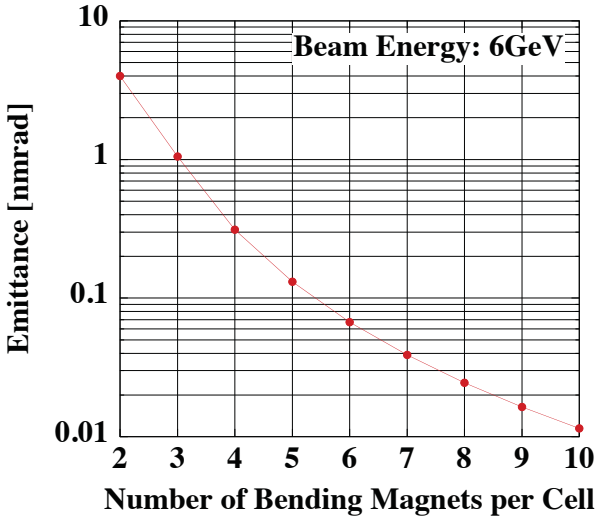

Figure 5.4: Typical values of the emittance for the SPring-8 storage ring calculated by assuming a multi-bend achromat optics and the same cell length. The beam energy is 6 GeV and the ring circumference is fixed at the present value of 1436 m.

Long Straight Section

In the SPring-8 storage ring there are four magnet-free long straight sections (LSS's). A quarter of the ring is composed of 11 unit cells and one LSS. Since the betatron functions at normal straight sections are set to be small, being about 1 m in both horizontal and vertical directions as shown in Fig. 5.5, we will use one of the LSS's for beam injection by extending the present beam transport line by about 170 m. The LSS has a simple lattice structure composed of weak qudrupole magnets to suppress local chromaticites in this section. The betatron phase advance in LSS is set to be $2\,\pi n$, where n is an integer, and so the LSS becomes "transparent" and the betatron functions at both ends are automatically matched to the unit cell. The straight section having a large horizontal betatron function is used for the beam injection. The rest can be used to install damping wigglers to control the beam emittance. When necessary in the future, other devices can also be installed in these sections.

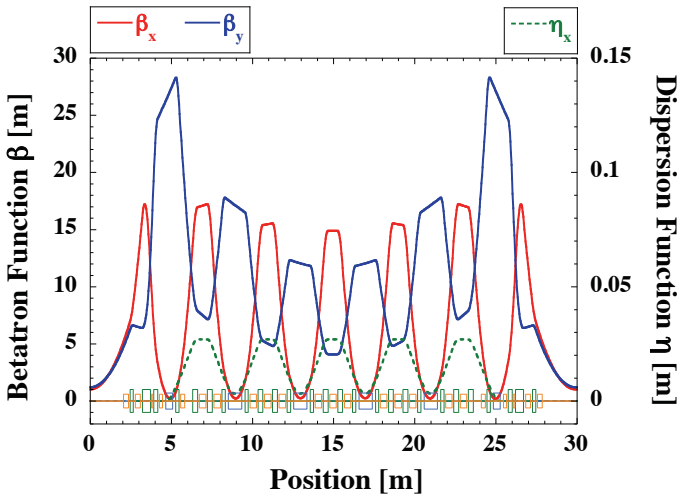

Figure 5.5: 6 bend lattice. The lattice functions and magnet arrangement (blue: bending, green: quadrupole, orange: sextupole) are shown.

Dynamic Aperture

As mentioned above, when we increase the number of bending magnets to achieve a smaller emittance value, the natural chromaticities become large, especially in the horizontal direction, and strong sextupole magnets are required for the chromaticity correction. Then the dynamic aperture shrinks and the momentum acceptance becomes small, and it becomes difficult to inject a beam with high efficiencies and to keep a stored current constant even in the top-up operation. To solve this problem and enlarge the dynamic aperture, we developed a method of optimizing sextupole strengths [12] by using an isolated resonance Hamiltonian [15] so that resonance excitations are suppressed for both on- and off-momentum electrons. In the optimization procedure we also took account of the high-order (nonlinear) dispersions [16] and chromaticities [17] to keep the momentum acceptance as large as possible.

We further incorporated an idea that dominant effects of nonlinear sextupole fields cancel when the betatron phase relation is properly set. In the unit cell of the 6 bend lattice the horizontal betatron phase between two bending magnets is close to π, and one can arrange sextupole positions and strengths so that their nonlinear effects cancel to a certain extent as in the case of (non-)interleaved sextupole scheme [18–20]. This scheme of cancellation can also be applied to the case between cells [11]. In our case the strengths of some sextupole magnets in the arc were fixed according to the former cancellation scheme, and the betatron phase advance of the unit cell was optimized according to the latter scheme: the horizontal tune difference is $\Delta\nu_x = 12.527$ per 4 cells and the vertical one is $\Delta\nu_y = 1.557$ per 2 cells, or $\Delta\nu_x = 35.450$ and $\Delta\nu_y = 9.563$ for a quarter of the ring (superperiod of the lattice structure of the whole ring). Though the cancellation of sextupole fields is not perfect, we found this is effective for maximizing the dynamic aperture.

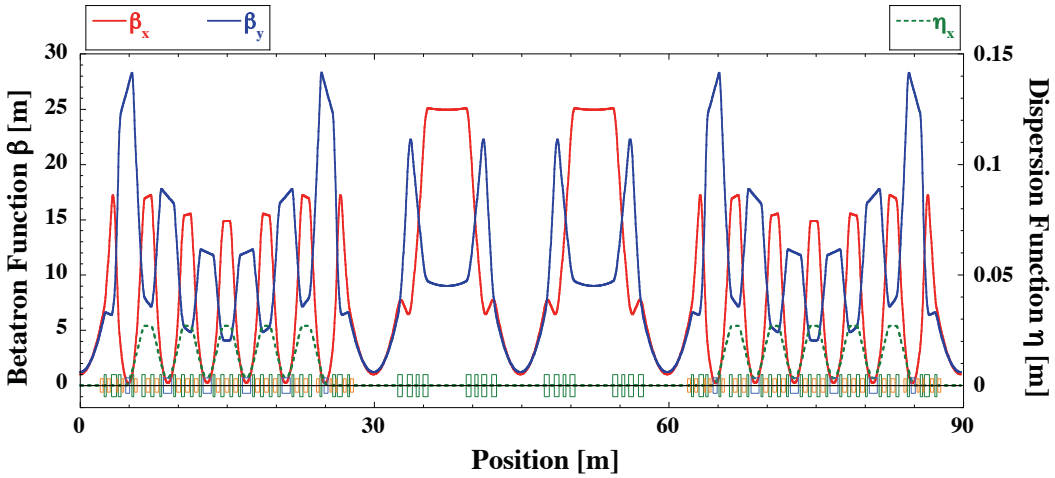

Figure 5.6: Typical lattice functions for three cells including the LSS (middle). In this example the betatron phase advance of the LSS is 2π in both horizontal and vertical directions.

In Fig. 5.7 we show the dynamic aperture calculated at the high-beta section of LSS. Since the sextupole magnets are strong, the dynamic aperture is sensitive to the sextupole misalignment. We checked the dependence of the dynamic aperture on the sextupole misalignment and found that the tolerance is about 10 μm. It is then needed to develop a very precise alignment and correction method. For checking magnet misalignment and for calibrating beam position monitors in the early stage of the beam commissioning, a "detuned" (or relaxed) optics having weaker quadrupole strengths will be useful. Since the sextupole magnets are also weaker in this optics, the dynamic aperture is robust against machine errors. Examples of such a "detuned" optics have been obtained, and these will be refined and used in discussing the commissioning scenario.

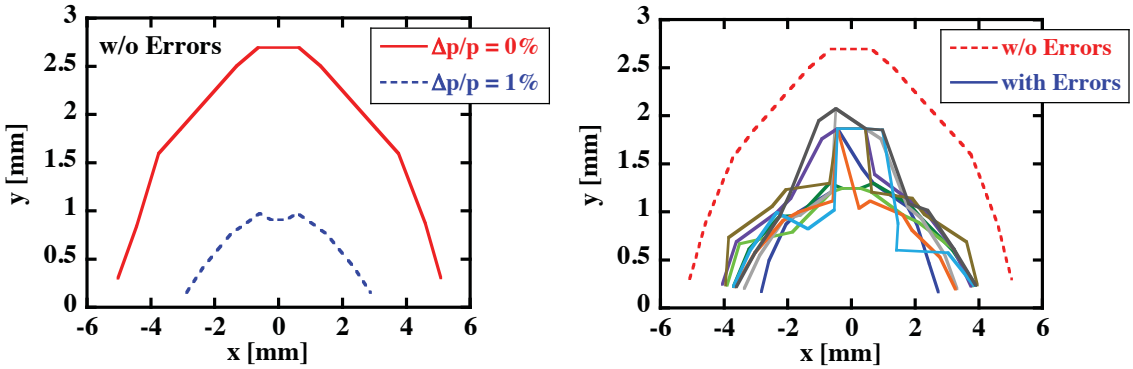

Figure 5.7: The dynamic aperture for the ideal ring without errors (left) and for the ring with sextupole misalignment (right) calculated at the high-beta section of LSS, where β_x = 24.9 m and β_y = 9.0 m. The sextupole misalignment was distributed according to the Gaussian distribution of σ = 5 μm with the cutoff at 2σ.

The momentum acceptance is about 2 % (see Fig. 5.7) and the Touschek beam lifetime is calculated to be about 0.1 h at the bunch current of 0.1mA and the emittance coupling ratio of 2%. To increase the beam lifetime and to relieve the intrabeam scattering effects, we plan to introduce a harmonic cavity system that allows us to control the bunch length.

Main parameters of the new storage ring are summarized in Table 5.1, where we also show parameters for the present ring for comparison.

Table 5.1: Main parameters of the storage ring.

	New Ring	Present Ring
Lattice Type	6 Bend	Double-Bend
Unit Cell Length [m]	29.92	29.92
Ring Circumference [m]	1435.95	1435.95
Beam Energy [GeV]	6	8
Natural Emittance [pm.rad]	67	3400
Energy Spread [%]	0.096	0.109
Dispersion Func. [m] at Straights	0	0.107
Betatron Func. [m] at Straights (H/V)	1.0 / 1.2	22.6 / 5.6
Betatron Tune (H/V)	141.80 / 38.25	40.14 / 18.35
Natural Chromaticity (H/V)	-473 / -199	-88 / -42
Momentum Compaction Factor	1.55×10^{-5}	1.68×10^{-4}
Radiation Loss [MeV/turn]	4	9
Number of Magnets per Cell (Bending / Quadrupole / Sextupole)	6 / 26 / 23	2 / 10 / 7
Bending Field [T]	0.70	0.68
Max. Strength of Quadrupoles [m^{-1}]	1.52	0.40
Max. Strength of Sextupoles [m^{-2}]	120	6.2

Damping by Insertion Devices

As we lower the beam energy, the damping effect due to insertion devices on the emittance is enhanced. This is demonstrated in Fig. 5.8, where the emittance (left axis) and the relative energy spread (right axis) is plotted as a function of the field strength of undulators installed in the normal straight section. We assumed that the number of undulators is 28, the same number as in the present situation at SPring-8, and they are all cryo-undulators of the same planar type having a period of 14.4 mm and a length of 3 m. By changing the gap of the undulators, one can vary their magnetic field up to 2.04 T, which corresponds to the photon energy of 5 keV.

From Fig. 5.8, we see that as we close the gap, the emittance is drastically reduced. When users require the photon energy at around 5 to 10 keV (indicated by dashed lines in the figure), the emittance will be around 30 pm.rad. In the present case, the minimum emittance that can be achieved by the damping effect of undulators is about 23 pm.rad (when all of the undulators are operated at the minimum gap, or at the maximum field of 2.04 T).

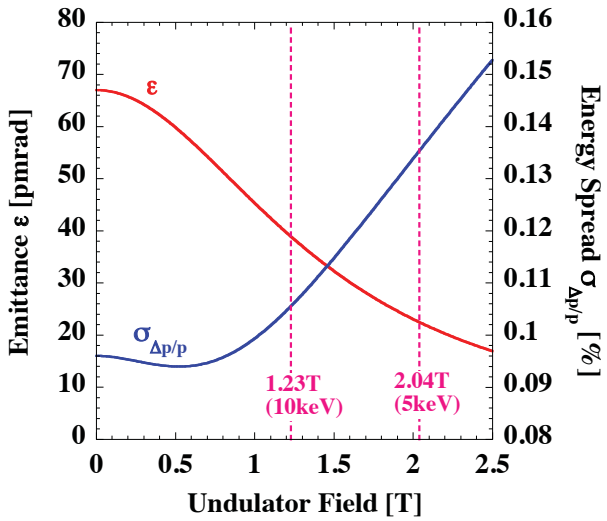

Figure 5.8: The effect of undulators on the emittance and the relative energy spread. In this calculation, 28 undulators, each having a period of 14.4 mm and a length of 3 m, are distributed in normal straight sections where $\beta_x = 1.0$ m and $\eta_x = 0$.

The emittance can further be reduced by using the damping wigglers. As shown in Fig. 5.6, the LSS has some magnet-free spaces and they can be used for installing damping wigglers. For definiteness, we assume that nine damping wigglers, each having a period of 50 mm and a length of 3 m, are installed in the low-beta sections of LSS and all of the undulators in the normal straight sections are operated at their maximum field of 2.04 T. Figure 5.9 shows the emittance and the energy spread calculated as a function of the magnetic field of the damping wigglers. As seen from this figure, the emittance of less than 20 pm.rad, being close to our ultimate goal of the "diffraction limit", can be obtained when the damping wiggler field is around 2 to 3 T.

The damping wigglers can also play another role in user operation: they can be used to keep the emittance constant when users change the gap of their undulators independently. Such a feed-forward control of the emittance will be important for keeping the light source performance during user operation.

5.2.2 Technology Developments

The basic lattice design for the upgraded SPring-8 has been overviewed in the previous section 5.2.1. The six-bend lattice has mainly been studied, for which linear and nonlinear optics

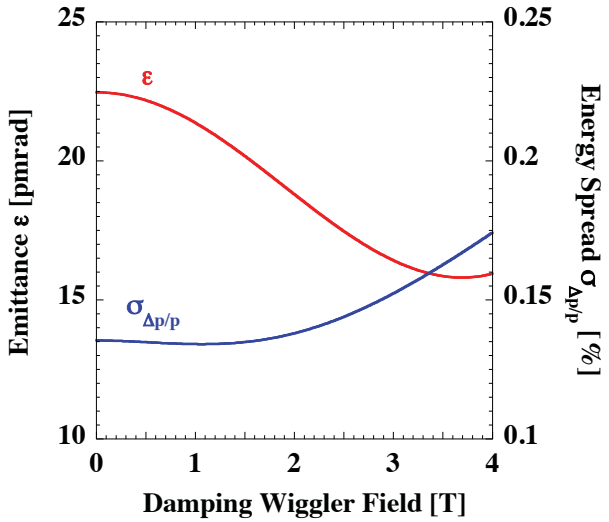

Figure 5.9: The effect of damping wigglers. In this calculation, nine damping wigglers are placed in the low-beta sections of LSS where β_x = 1.0m and η_x = 0. Each damping wiggler has a period of 50 mm and a length of 3 m.

have been optimized. The resulting performances as a light source are summarized in Chapter 6, which will presumably meet demands for future sciences. However, we have to verify the feasibility of the lattice in terms of technologies beforehand. It is especially because the lattice aims at the ultimate performance as a storage ring under several constraints. Such a challenging upgrade imposes not only an advanced lattice design via manipulation of nonlinear beam dynamics but also extensive technological developments in almost every component such as an injection device, magnets, RF systems, and monitors.

A design of an extremely small emittance ring naturally results in the following technical challenges. First, a dynamic aperture becomes smaller as natural chromaticities become larger and sextupoles that compensate it have stronger magnetic gradients. An injector, therefore, needs to accommodate such a small acceptance. Next, required magnetic fields for multipole magnets, especially sextupoles, will quickly increase as the number of bending magnets is increased. Thus, development of multipole magnets is one of key issues. As a combination of the two natures, i.e., small dynamic apertures and high magnetic gradients off an axis, an accuracy of sending electron beams in each magnet has to be very high. For the purpose, a monitor system attached to a magnet assembly needs further development. An intra-beam scattering (IBS) effect also comes into play. As transverse emittances are made small, the IBS effect starts to dominate the final emittance. To avoid it, RF systems should take care of a longitudinal bunch distribution of electrons to suppress the emittance blowup.

These technical challenges have been recognized in our design, too. It is no more reasonable for us to fix the lattice first, then develop hardwares afterward based on the lattice. Instead, it is frequently necessary to go back and forth between the lattice and hardware designs. Otherwise,

the feasibility of hardware is not secured.

Thus, the lattice design shown in the previous section is actually the consequence of the iteration process between the lattice design and the extensive hardware studies, although the hardware developments still have to be continued via R&D's. One good example is that the packing factor is so high and simultaneously the integrated magnetic fields of multipole magnets are so high that the magnets should be carefully distributed in order to avoid extremely high magnetic gradients that are technologically impossible. (The packing factor is the ratio of space occupied with magnets to the total.) The lattice design shown in Fig.5.6 already considers such an iteration. In the following, the requirements for technology developments and our approach to them are overviewed.

Injection Schemes

The first requirement for a design of the new injection system is to accommodate the small dynamic apertures presented in Fig.5.7. Under assumption that the sextupole alignment tolerance is ± 10 μm, dynamic apertures are estimated to be about 2.5 mm in horizontal and 1 mm in vertical directions at the betatron function of ~25 m. This aperture is ten times smaller than that of the current ring. Also the natural bunch length of the SPring-8 II ring is a few ps, one fifth of the current values of the rings. The injection to such small acceptances requires low emittance and short bunch beams from an injector.

The top-up operation is also an important feature for the injection system. Since the top-up operation was introduced to SPring-8 in 2004, the new type of injection has brought significant changes to user experiments. Heat loads on X-ray optics are kept stable, and flux at samples do not decrease any more as time elapses. Now the new feature is taken for granted, and should be maintained at the next ring. More precisely, we should satisfy the following strengths in terms of the injection system (in the order of appearance in the following):

(1) low injection beam loss to the narrow aperture for radiation safety and low damage on insertion device,

(2) a variety of filling patterns with a variety of bunch current,

(3) minimum perturbations on stored beam,

(4) a high purity single bunch; currently, the bunch purity of SPring-8 is in the order of 10^{-10} or a single electron level,

(5) a stored current stability of the order of 0.01 %.

The requirement on the beam parameters and candidates for the new injector are compared in Table 5.2. The booster synchrotron, i.e., the current injector to the SPring-8 ring, has large

emittance and long bunches that do not fulfill the requirements, unless large amount of efforts including budgets are to be put into the renewal. The SACLA linac, on the other hand, produces extremely high quality beam in emittance and bunch length with an adequate repetition rate. Therefore we choose the SACLA linac as the best candidate for the injector of the SPring-8 II. Although further discussion on the choice of the injector will be necessary, the parameters of the SACLA linac are expected to meet the requirement (1). For the same purpose, the injection point would be moved from the current injection point at the normal straight section to one of the four 25-m long straight sections (LSS). At LSS, the horizontal betatron function can be adjusted to be more than 20 m for a large dynamic aperture, while that at the normal straight sections is fixed at ~1 m for insertion devices. By choosing the SACLA linac and the LSS as the injection point, it is expected that the injected beams fit in the small dynamic apertures without significant losses.

Table 5.2: Parameters of candidates for injector

Parameters (rms)	Requirement	SACLA	Booster Synchrotron
Emittance	≤1 nm.rad	0.05 - 0.1.nm rad	100 nm.rad
Beam size at β_H = 25m	≤0.17 mm	0.035 - 0.05 mm	1.5 mm
Energy spread	≤0.2 %	0.1 %	0.1 %
Bunch length	≤10 ps ≤25-50 ps [1]	< 1 ps	< 60 ps
Repetition rate	a few Hz	60 Hz	1 Hz
Bunch charge	0.25 nC[2]	0.25 nC	> 0.25 nC

[1] with higher harmonic RF

[2] for 100 mA with on-axis injection

An off-axis injection is preferred for the requirement (2). SPring-8 has currently provided the bunch current of 3.0 mA at maximum, which corresponds to the bunch charge of 14.4 nC. Such a high charge needs to be built up by multiple injections at the same bucket via the off-axis injection. For the off-axis injection, the incident beam is guided to the aperture by an injection device, while the stored beam is kept in the aperture without being considerably affected. Since the expected dynamic aperture for the new ring is a few mm, the distance between the injected and the stored beams should be a little less than that. It follows that the strong position dependence of the kick field needs to be given by the injection device. Therefore well-known off-axis injection schemes with bump orbit formation are not necessarily appropriate, as far as we consider the requirements mentioned above. The pulsed quadrupole magnet [21] is one candidate for such an injection device. However, the scheme excites a quadrupole oscillation on stored beams, which lasts for the damping time after the injection.

Note that the pulsed field of a magnet lasts at least for several hundreds of nano-seconds due to its inductance, thereby all the stored beams during this period suffer the quadrupole oscillation. Although a counter pulsed quadrupole may solve this problem, the installation space at matched betatron phase and the precise adjustment of the strength and the pulse shape would be required. A pulsed sextupole may be another solution, because it is superior in regard to the quadrupole oscillation due to no quadrupole field at the stored beam. Nevertheless, the question is whether it is feasible to manufacture such a magnet for matching the small dynamic aperture like our case; it would require very strong sextupole fields to deflect incident beams, leaving stored beams unkicked just a few mm away. Thus, the schemes with pulsed magnets do not seem to fulfill the requirement (3) in our case.

As a result, we propose to introduce a new injection scheme based on a bucket-by-bucket injection (BBI) using a variable field fast kicker [22]. The fast kicker is composed of two stripline electrodes and each is excited with a TEM mode by a high pulse power driver. The fast kicker produces a deflecting field with a time duration of about 3-4 ns, which can separate only one bucket from adjacent buckets that are separated by 2 ns. The length of the kicker is 0.2-m long for fast kick pulse, thus several kickers will be installed to the ring to obtain necessary amount of kick for the injection.

The fast kicker is designed such that the kick field can be continuously controlled from dipolar to quadrupolar field by adjusting the power and polarity of the input to the kicker. With the quadrupolar kick field, the injection beams are guided to off-axis of the fast kicker where there is a quadrupole-like deflecting field, while store beams feels no significant deflecting field on the axis as in Fig.5.10 . Although the quadrupolar field on the axis excites the quadrupole oscillation on the store beam, it only occurs in one bucket that are being injected. Thus, the quadruple oscillation is no more a problem and the requirement (3) is fulfilled. Also, with BBI scheme, the satellite bunches in injection beams are naturally rejected by the fast kicker as expected and the requirement (4) should be fulfilled by the BBI scheme. The requirement (5) will be maintained as far as the new injection system including the new injector catch up with the required repetition rate (~3 Hz) estimated by the beam lifetime.

Here, we would like to emphasize one more important feature for the new injection system. We find it important to prepare an option of on-axis injection. Since the dynamic aperture is expected to be small, the on-axis injection can be very effective especially at early stages of commissioning, or for some advanced operations in the future. The concept of taking advantage of the on-axis injection for the small dynamic aperture is referred as "swap-out" coined by the APS [23]. Note that we designed the BBI fast kicker so that the apparatus also enables a *bucket-by-bucket* on-axis injection by changing kick fields inside the fast kicker to dipolar field. The scheme is schematically drawn in Fig. 5.10. Only the single apparatus can switch between on- and off-axis injections, both of which work for a single bucket. It is another advantage of the

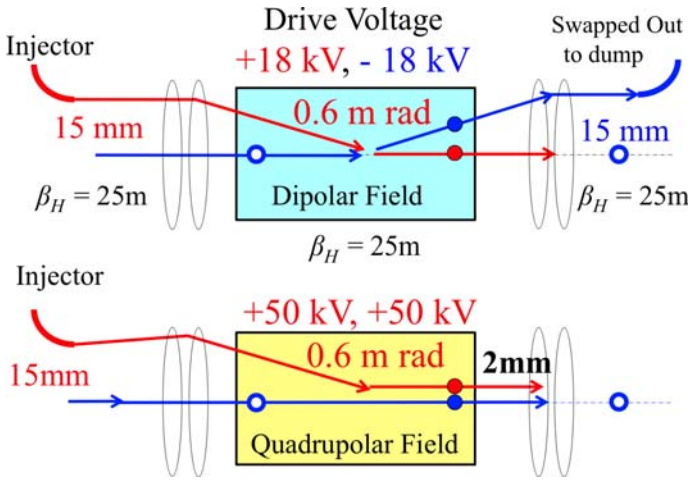

Figure 5.10: Top: On-axis injection with dipole kick by fast kicker (boxes). Bottom : Off-axis injection with quadrupole kick. The kickers are excited just at the injection bucket.

BBI fast kicker compared with pulsed multipole magnets.

The prototype of the fast kicker is now under construction for the feasibility study of the BBI injection scheme [1].

Magnet System

A magnet configuration in a cell of the newly designed 6 bend lattice is drawn in Fig.5.11. The magnets marked ”B” and ”D” are dipole magnets, where ”B” has a half length of ”D”. Quadrupole and sextupole magnets are distributed in segments ”A”, ”C”, ”E”, and ”F”. Some space is found in segments ”C”, where we are considering a possibility of installing mini-undulators. The new lattice does not only need three times more bending magnets than the existing lattice has, but also a lot more quadrupole and sextupole magnets in between. Moreover, the integrated field strengths of quadrupole and sextupole magnets intrinsically become much higher than the present ones as we proceed to the extremely small emittance ring (see Table 5.1). The issue in regard to the strong multipole magnets as well as the high packing factor is one of the common challenges in developments of extremely small emittance ring. It is obviously the case for us, too.

Our first approach is to define acceptable minimum distances between neighboring magnets for the lattice design. By that, we can take full advantage of extending longitudinal magnet lengths that helps mitigate the field gradient of each magnet. In order to determine the minimum distances, it is assumed that an overlap of magnetic fields from two neighboring magnets in a drift space in between is to be accepted, if necessary. Meanwhile, a significant intrusion of

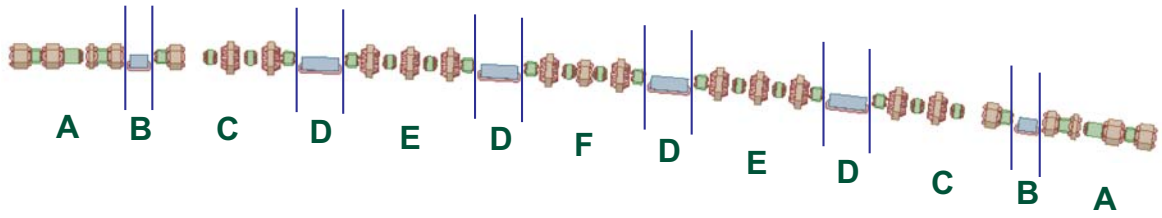

Figure 5.11: A magnet configuration design for a normal cell (*color*). In this figure, *blue*, *green* and *brown* magnets represent dipole, quadrupole and sextupole magnets, respectively. None of steering magnets are drawn in the figure. Electron beam propagates from right to left.

magnetic field from one magnet into the other should be avoided. Also, the magnets that are close with each other are carefully designed so that the total length of each magnet including coils and its support should not exceed that of the core itself [1].

Throughout such an iteration between the lattice and magnet designs, the lattice has been fixed at the moment as presented in Section 5.2.1 and drawn in Fig. 5.11. The resulting maximum field gradients of sextupole magnets are estimated to be somewhere between 10,000 and 14,000 T/m^2, which is still high. Taking vacuum enclosures into consideration, we define a bore diameter as 26 mm. Good field regions of all the magnets are designed to be ±3 mm both in horizontal and vertical directions because the dynamic aperture of the ring is estimated to be approximately ±2 mm in horizontal, and ±1 mm in vertical axes (Fig.5.7). The specifications and total numbers of dipole, quadrupole, and sextupole magnets are summarized in Table 5.3.

Since the required magnetic fields listed in Table 5.3 are high, even if a shape of a magnetic pole is optimized with a pure iron (e.g., JIS C 2504 SUY-0), field saturation in the core cannot be avoided. Thus, unique core materials are required to avoid the saturation in a core.

Saturated magnetic flux density of an iron alloy with cobalt is much higher than that of the SUY-0. Field calculation for multipole magnets are performed and are compared by using the code ”MAFIA” for two core materials, an ideal magnetic iron alloy, ”Steel1010”, and the Co-Fe alloy. As discussed in detail in Ref [1], the Co-Fe alloy is adopted as a possible magnet core material for high gradient quadrupole and sextupole magnets, and R&D, including an optimization of mixing rate of cobalt, is planned.

As a consequence, there is no plenty of space prepared for steering magnets. Some quadrupole magnets may function as steering magnets by attaching extra coils. The maximum kick angle is designed to be 0.5 mrad both in horizontal and vertical directions.

The alignment of magnets, especially that of sextupole magnets, is also one of the most critical issues for verifying the feasibility of the new ring. As discussed in Section 5.2.1, it is critical to keep a closed orbit in the vicinity of the center of sextupole magnets; otherwise, the dynamic aperture considerably shrinks to prevent orbiting beams from being stably stored.

Table 5.3: Specification and total number of dipole, quadrupole, and sextupole magnets

Parameter	Dipole	Quadrupole	Sextupole
Center field	0.7 [T]	36-50 [T/m]	<14,000 [T/m^2]
Length [m]	0.41,0.82	0.2–0.5	0.1–0.4
Gap or bore size [mm]	26	26	26
Good field region [mm]	±3	±3	±3
Field tolerance	10^{-4}	10^{-4}	10^{-4}
Total number	264	1144	1012

According to Fig. 5.7, the tolerance, that is an acceptable error between the closed orbit and the sextupole magnetic center, has to be ±10 μm or less in both horizontal and vertical directions. In order to solve the issue, we need to develop an integrated strategy including the alignment scheme of magnets and commissioning procedures. Up to now, several scenarios have been proposed and discussed. The discussion on the integrated strategy is summarized in the section of Diagnostics and Instrumentations below.

Vacuum System

The new ring would be operated at a top-up mode as the current SPring-8 is. Yet, it would be important to sustain a reasonable beam lifetime in order to meet the requirement on the current stability. Another advantage of the long lifetime is that the beam current does not quickly decrease while some mechanical or other problems interferes the top-up operation. As discussed in the section of RF system, the Touschek lifetime is expected to be around an hour, which is close to the lowest accepted for the stable top-up operation. Therefore, it is required that the vacuum lifetime, i.e., the beam lifetime determined by vacuum conditions, should be enough longer than the Touschek lifetime so that the overall lifetime is not significantly deteriorated from the Touschek lifetime. Another concern for the vacuum system is that a bore radius of magnets is 26 mm at minimum due to high magnetic fields required for the low emittance lattice. Thus, considerably thinner vacuum chambers than the present ones have to be developed for securing enough height of light slots.

The vacuum related beam lifetime is described by cross sections, and is mainly contributed by the three factors; 1) Rutherford scattering : σ_r, 2) Møller scattering : σ_m and 3) Bremsstrahlung : σ_b; $\sigma(Z_i) = \sigma_r(Z_i) + Z_i\sigma_m + \sigma_b(Z_i)$. Electron beam will be annihilated in vacuum ducts if the orbiting electron scatters with an angle of above a critical value ϕ_c or above a critical energy loss γ_c. In general, H_2 and CO are considered to be dominant residual gas components in pre-baked vacuum ducts during operation.

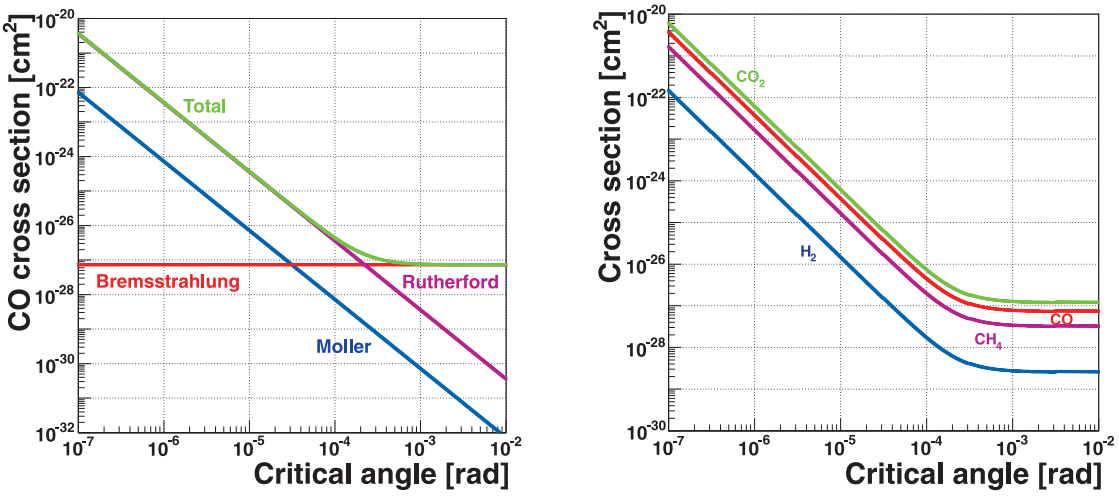

Figure 5.12: Calculated cross sections of the electron scattering with CO molecule (*left*) and with prominent residual gas molecules (*right*). An electron energy of 6 GeV is assumed.

Figure 5.12 represents calculated cross sections of the electron scattering with CO molecules (*left*) and with prominent residual gas molecules, H_2, CH_4, CO and CO_2 (*right*) assuming the electron energy of 6 GeV. It is found that the Rutherford scattering is the major factor to determine the lifetime when a critical scattering angle is less than $\phi_c \sim 10^{-4}$ rad. As shown in Fig. 5.12 (*right*), the cross section becomes smaller as the atomic number (Z_i) of the scattered residual gas particle becomes smaller. Electron beam lifetime, τ_i [s], which is caused by the scattering with a residual gas atom (Z_i) is described as

$$\frac{1}{\tau_i} = cn_i\sigma(Z_i) = c\frac{P_i}{k_B T}\sigma(Z_i), \tag{5.2}$$

where P_i residual gas pressure in Pa, n_i density in m^3 and T temperature in K. k_B is the Boltzmann constant, 1.38×10^{-23} J/K. The minimum critical angle for the new ring discussed in Section 5.2 is estimated to be 8×10^{-5} rad. Figure 5.13 summarizes the relation between the vacuum lifetime and the partial pressure for the individual four residual gas components; H_2, CH_4, CO and CO_2 at $\phi_c = 8 \times 10^{-5}$ rad.

From Fig. 5.13, it is found that a reasonably achievable beam lifetime is estimated to be around 10^5 sec., i.e. 28 hours, under assumption that the reliably achievable pressure is a fraction of 10^{-9} Pa. Now a contribution from the Touschek effect to the beam lifetime (τ_t) is estimated to be about an hour under the assumption that an appropriate RF system functions as a bunch stretcher. Therefore, assuming that the total beam lifetime (τ) is determined by the vacuum system and the Touschek effect, the total beam lifetime is

$$\frac{1}{\tau} = \frac{1}{\tau_v} + \frac{1}{\tau_t} \rightleftharpoons \tau \cong 0.97 \quad \text{[hours]}, \tag{5.3}$$

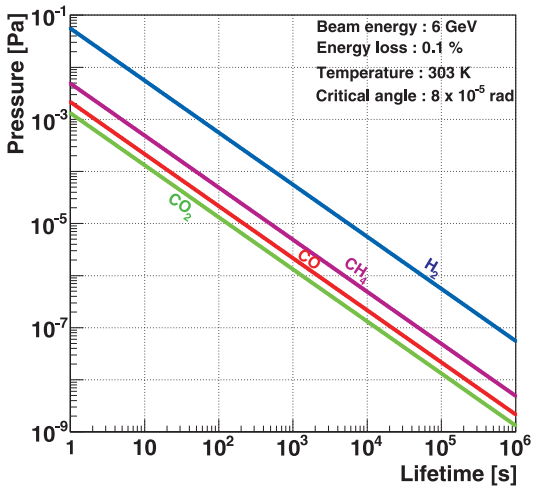

Figure 5.13: Calculated electron scattering cross sections and partial pressures for four prominent residual gas molecules. Electron energy of 6 GeV, energy loss (γ_c/γ) of 0.1 %, and temperature of 303K are assumed.

which is not significantly smaller than the original Touschek lifetime as expected. As an option, the longer Touschek lifetime, such as 3 hours, is also considered via an adjustment of the coupling ratio, especially in a commissioning stage. In the case, the overall lifetime is estimated to be 2.7 hours according to Eq.(5.3).

RF system

The role of an RF acceleration system of a storage ring is to generate a sufficient beam-accelerating voltage and compensate for beam energy loss caused by synchrotron radiation at bending magnets and insertion devices. The RF system of the current SPring-8 storage ring has stably generated a voltage of 16 MV at a frequency of 508.58 MHz and accelerated electron beams with a current of 100 mA [24].

In upgrading the storage ring for the SPring-8 II, a beam energy would be lowered to 6 GeV but a beam current would be increased up to 300 mA. Radiation losses at bending magnets, undulators and damping wigglers are respectively estimated to be 4.0, 2.0 and 4.0 MeV/turn, so the total is 10 MeV/turn. In practical user operations in the future, we plan to keep the total radiation loss at 8 MeV/turn by adjusting damping wiggler gaps depending on the status of insertion devices. The reason is that an equilibrium emittance with radiation dampings should be constant irrespective of user settings of insertion devices. Thus, the possible radiation loss ranges from 8 to 10 MeV, and we suppose the new RF system should be able to provide the accelerating voltage of 16 MV as a possibly maximum value that we have to care. In terms

of the RF frequency, the same frequency as the current one, 508.58 MHz, is chosen. Refer in detail the section of timing system below.

New RF stations for the acceleration would be distributed at three normal straight sections. The normal straight section is 4 m long each (Section 5.2.1), so the whole length of the RF cavities at each station has to be no more than 4 m in total including the whole assembly. The existing cavities in the SPring-8 storage ring does no more fit in it. Further, the increased stored current excites strong coupled-bunched instabilities from impedances of parasitic resonant modes, while the current RF cavities in SPring-8 ring have no countermeasure for the strong instabilities [25]. Thus, we have designed a new RF cavity that meets the new requirements. The TM020 mode is selected as a beam-accelerating mode since it has a shunt impedance sufficient for the beam acceleration. The shunt impedance is 6.8 MΩ and a beam-accelerating voltage of 16 MV is generated with 24 cavities, i.e., 8 cavities at each station. The TM020 mode also enables a compact damping structure for the harmful parasitic resonance. The detailed design is presented in Ref. [1].

Table 5.4 summarizes the major parameters for the new RF system. The accelerating voltage of 16 MV and the shunt impedance of 6.8 MΩ at 24 cavities result in the total cavity-wall loss of 1.6 MW. The stored current of 300 mA and the accelerating voltage of 10 MeV/turn correspond to the beam loading of 3.0 MW. In consequence, it is required to supply RF power of about 5 MW with the RF cavities. The requirement for RF power sources is again beyond the capability of the existing ones. For the sake of cost-effectiveness and a smooth transition from the current to the new systems, we are going to reinforce the existing power sources, instead of replacing with completely new ones. The total power of 5 MW will be supplied by six klystrons, each of which will have a rated output of 1 MW, an efficiency of better than 60% and a gain of more than 50 dB. Two klystrons will be situated at each station, and each klystron drives four cavities (i.e., 8 cavities per station). Correspondingly, the power supplies will be upgraded so that each can be enough to drive two 1 MW klystrons. The DC power supplies should have a voltage ripple of less than 0.5 % peak-to-peak to decrease the noises on the RF power output from the klystrons.

The coupling between an RF cavity and an external waveguide circuit must be adjusted in order not to cause a useless power-reflection from the cavity with variable beam loading. We have been developing a new RF input coupler with a coupling tuner to avoid coupling discrepancy. The optimum coupling coefficient of the SPring-8 II cavity is 2.9 at a beam current of 300 mA. The tuner will cover the necessary coupling range and be adjusted according to the various beam current without interrupting the continuous RF feed [1].

In order to achieve the diffraction limited beam both in the horizontal and the vertical directions, it is crucial to avoid the emittance growth due to the intra-beam scattering (IBS).

Table 5.4: Main parameters of fundamental RF system.

RF frequency [MHz]	508.58
harmonic number	2436
energy loss [MeV/turm]	10.0
at bending magnets	4.0
at undulators	2.0
at damping wigglers	4.0
acceleration voltage [MV]	16
RF accelerating stations	3
1 MW klystrons	6
RF cavities	24
total cavity-wall loss [MW]	1.6
beam loading power [MW]	3.0

Figure 5.14 shows the dependences of the emittance growth and the beam lifetime on the bunch length. The emittance grows remarkably and the beam lifetime becomes short as the bunch length reaches a natural length of about 5 ps. It is essential to lengthen the bunch longer than 20 ps in order to mitigate the IBS and keep the low emittance as well as enough beam lifetime. We, therefore, plan to introduce a 3.5th harmonic system for the bunch lengthening at another RF station. Because a harmonic voltage needs to be about 3.5 MV at a beam accelerating voltage of 16 MV, we would use two super-conducting single-cell cavities resonating at 1780.03 MHz. Table 5.5 shows the parameters of the harmonic cavity. The cavities should be operated at 2 K in temperature, and their wall loss would be reduced to about 4 W.

Table 5.5: Parameters of the Harmonic Cavity

frequency [MHz]	1780.03
harmonics	3.5
mode	TM010
unloaded Q	10^9
R/Q [Ω]	80
Number of cavity	2

Two types of cavity operations are under consideration: (1) active operation driven by an external RF power source and (2) passive operation driven by a beam-induced power [27].

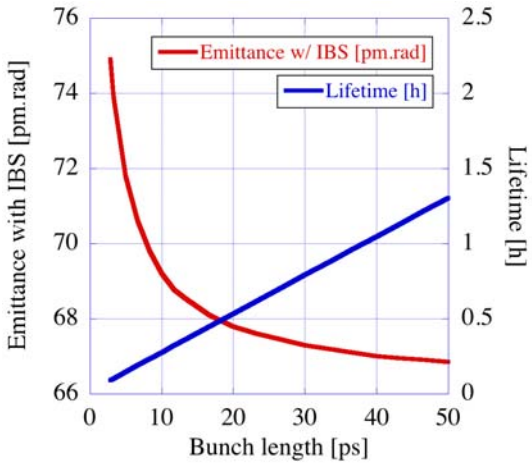

Figure 5.14: Dependence of the emittance and the beam lifetime on the bunch length. (elegant calculation [26] at a bunch current of 0.1 mA)

Figure 5.15 shows the bunch lengths in the active and the passive operations by the double RF model calculation [28]. In the active operation, the bunch extends to 50 ps and becomes 10 times longer than the natural bunch length. In order to succeed the active operation, however, an RF system must have stabilities of less than 0.1 degree in phase and of less than 1% in voltage. In the passive operation, a bunch length can be extended to 25 ps or more. The resulting bunch length is half of that obtained in the active operation, but is sufficient to meet the minimum requirement that the beam lifetime should be over half an hour. No external RF components other than the super-conducting cavities are necessary, so the RF system becomes simple and inexpensive. Since a frequency tuner is the only knob to control the cavity voltage, the passive operation is less flexible than the active operation, though.

Due to the harmonics of multiples of half integer, we can simultaneously compress a beam to a length of 4 ps and store long and short bunches bucket by bucket (Section 5.3). Damping higher-order-modes (HOM) in the cavity and 2 K cooling system are the matters with both the active and the passive operation. We should develop a HOM coupler or a HOM absorber that are fit to the cavity in a cryo-module and construct the cooling system.

Diagnostics and Instrumentations

One of the most challenging issues in technology developments for the SPring-8 upgrade is to develop new diagnostics that enable a precise observation of an electron orbit at each magnet position. In the following, the challenging issue is first addressed, then our strategy to approach the issue is presented.

As shown in Fig. 5.7, the alignment error of sextupoles must be less than ±10 μm. Otherwise, the dynamic aperture of the ring shrinks and there is a chance that the beam is no more

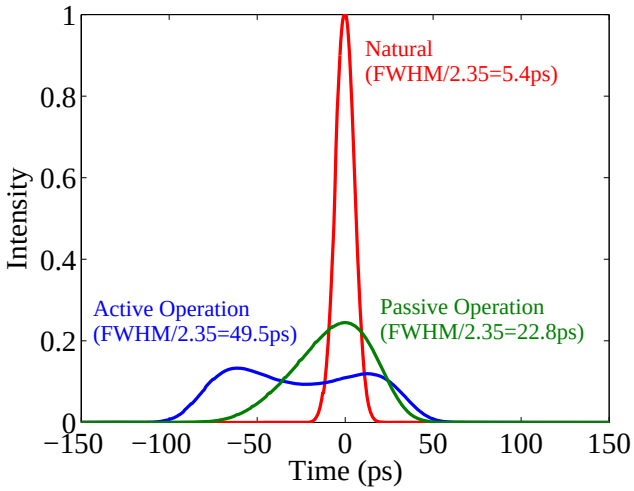

Figure 5.15: Calculation of the bunch lengthening in active and passive operations of the harmonic cavity.

stored. Note that even if the initial alignment of magnets is imperfect, say, the initial random errors of sextupole magnets are more than ±10 μm, the beam is still able to be stored as far as the electron orbit is properly guided to the center of each sextupole within the tolerance in a beam commissioning. Therefore, the challenging issue is how we should integrate the whole strategy, including not only the alignment of magnets but also the commissioning procedure, to guide the electron orbit to the center of all sextupoles within the tolerance.

Our first strategy to approach the issue is to align neighboring magnets as precisely as possible by making use of a vibrating wire technique [29] and others. Note that not only sextupole but also quadrupole magnets need to be precisely aligned to some extent in our case, because undesirable dipole kicks from the off-axis field of the strong quadrupoles may produce an unacceptable closed orbit distortion for the initial commissioning [1]. The bottom line is that magnets should be aligned as precisely as possible whatever the following commissioning procedure is. Based on our experience with the current SPring-8 and the results at other sites, we expect to achieve about the same order of accuracy as required ($\sim \pm 10$ μm), but still need a backup. Further, the initially aligned magnets may eventually move due to temperature shift or other drifts in circumstances.

Therefore, the second strategy is to prepare beam position monitors (BPM's) that allow us to measure *absolute* beam positions against magnetic center of each sextupole. We mean by the term "*absolute* beam position" that precise measurements of relative positions, or movement, of beam positions are not enough. We have to precisely know the relation between the center of magnet and the BPM position, so that beam positions against the magnetic center are to be measured with an adequate resolution. This capability enables us to adjust an electron orbit to the magnets, either in commissionings or daily operations.

The accuracy of the *absolute* beam position measurement is determined by a convolution of several factors, such as residual errors in the BPM calibration, a nominal (instinsic) spatial resolution of BPM, and systematic error like beam current dependence of electronics. In addition, mechanical stability of BPM chambers and electrodes as well as the stability of BPM electronics are also essential to sustain the precise absolute measurement in continuous operation. An overall resolution contributed by these factors has to be kept below as small as ± 10 μm, unless another approach to meet the requirement, such as a new commissioning scheme, would be introduced.

Another scenario of the commissioning may be to observe tune shifts due to the off-axis field of sextupoles, since the tune shift is more sensitive to the misalignment than the position shift is. The challenging issue is still under consideration and more confirmation is needed. Detailed monitoring schemes as well as commissioning strategies are further discussed in Ref. [1], or will come later.

BPMs would be equipped not only nearby sextupoles but also on both sides of insertion devices and long straight sections. The number of BPMs for SPring-8-II is listed in Table 5.6.

Table 5.6: The number of BPMs for SPring-8-II

Sextupole	1012
ID sides	120
LSS	16
Total	1148

In addition to the BPM system, varieties of instruments, such as current monitors, beam size monitors and bunch length monitors, are indispensable for reliable and stable beam operations. At the same time, reuse of instruments of the SPring-8 facility is also important from a perspective of cost effectiveness and environmental consideration. Since developments of these monitors other than the BPM are unlikely critical, existing instrumentations would be reused as far as it is possible.

New vacuum enclosures and in-vacuum insertion devices will have smaller apertures than the existing ones. It results in larger resistive wall impedance and other collective effects, which may cause transverse and longitudinal instabilities of beams. We have been developing a transverse bunch-by-bunch feedback system based on a new concept in order to overcome the high growth rate of the multi-bunch and single-bunch instabilities [1].

Timing Systems

As discussed in the previous chapters, the synergy of the new storage ring and the XFEL is one of unique features for the upgrade plan. The electron beam is planned to be injected from the XFEL linac to the new storage ring, and pump-and-probe experiments using X-rays provided from the two extreme light sources are supposed to give new opportunities to users. For the purpose, it should be made sure that the two light sources work together.

One of concerns is that master oscillators of the two accelerators have different frequencies; the XFEL linac is based on 2,856 MHz and other sub- and higher harmonics such as 5,712 MHz (C-band), whereas the new storage ring is designed on a 508.58 MHz basis. It should be emphasized that the situation on the frequency relation exactly happens at the current storage ring of SPring-8 and its injector. The current storage ring and the booster synchrotron are operated at 508.58 MHz, while the linac runs on a 2,856 MHz basis. Yet, a precise injection timing system from the injector to the ring successfully functions (see Ref. [30].) It is therefore expected that the similar timing system should work for the new coupling between the SPring-8 II and the XFEL linac, although further study continues.

A timing jitter is one of important issues for the design of timing systems. An acceptable timing jitter is first determined by a length of injection bucket. As described in the section of RF system, superconducting harmonic cavities are installed in order to simultaneously store short and long bunches. Since the resulting bunch length of the short one is 4 ps, the requirement for the timing jitter should be a fraction of the bunch length. Another factor that may limit the timing jitter is a requirement for pump-and-probe experiments. An overall time resolution of the pump-and-probe experiment is determined by a convolution of pump and probe pulse lengths and the timing jitter in between. Thus, it is again desirable to suppress the timing jitter below the pulse lengths. As a result, we set a goal that the timing jitter should be a few picosecond or less.

The timing jitter of the injection system is not only generated from its electronics and related devices, but also from that of synchronous phase, at which electron bunches stays as a result of radiation damping and RF acceleration. Since the synchronous phase changes as gaps of insertion devices are independently altered by users, or accelerating voltages are shifted by bunch charge fluctuation, it is also demanded to adjust a beam injection timing based on a measurement of actual bunch arrival time.

Since the accuracy of timing system in the order of a few picosecond is generally not brand-new in today's accelerator technologies, we expect that such a timing system would be feasible with existing technologies. Further study and development will continue [1].

5.3 Short Pulse Options

Short pulse options are prepared for time-resolved experiments of pico-second order and fast pump-and-probe experiments with high repetition rate. Short X-ray pulses from a storage ring have very wide spectral range and would allow us to observe dynamic evolutions of microscopic systems in various time scales from pico- to several seconds. Basic strategies of short X-ray pulse generation have been considered as follows:

(1) A target pulse width is in a range of subpico- to pico-second.
(2) Only selected bunches are shortened, leaving others untouched to avoid deterioration of the ultra low emittance. (see Fig. 5.16)
(3) Short X-ray pulses are available at all beamlines.

Subpico- to pico-second X-ray pulses are expected to fill a gap of almost three orders of magnitude in bunch lengths between several tens of femtosecond available by the SACLA linac and several tens of picosecond by the SPring-8 II. In addition, the time range of pico-second or less will be of essential importance for temporal resolution of novel pump-and-probe experiments such as a method using synchronization with SACLA called X-ray pump and X-ray probe experiments (see Chapter 4).

Figure 5.16: Short bunches are trapped in some specific buckets. Other buckets are dedicated for long bunches with the ultra low emittance.

As methodologies to generate short X-ray pulses at a storage ring, there are two types of schemes; bunch compression and bunch slicing. In general, the former is supposed to yield higher peak brilliance/flux than the latter does, because the slicing schemes extract a part of a pulse energy. The slicing, on the other hand, may enable us to generate shorter radiation pulses, some of which are even synchronized with external laser pulses. More precisely, the two types of schemes may differently affect the transverse emittance, energy spread, and other characteristics of stored beams, especially for a very low emittance ring. Note that the combination of the compression and the slicing may also work. Thus, it is necessary to thoroughly study what is a best option to generate short X-ray pulses at the upgraded SPring-8.

The bunch compression in the subpico-second range requires a very strong RF potential

to confine all electrons of a bunch. The RF potential needs to have the frequency of mm-wave range and a peak power of Giga-watt level to beat a wake potential derived from the coherent synchrotron radiation (CSR). One possible solution to apply the strong confinement potential to the electron bunches may be a mm-wave inverse free electron laser (mm-iFEL) [31] as discussed in the supplementary volume [1]. Simulation studies show that the mm-iFEL leads to the equilibrium bunch length of 0.6 ps (r.m.s.), when a bunch charge is 479 pC corresponding to a bunch current of 0.1 mA.

Another way to compress bunches is to make use of the higher harmonic RF system. Though the system is mainly supposed to lengthen stored electron bunches by modifying the main RF potential, it can also be applied to shorten the bunches once the RF phase of the higher harmonic is optimized for bunch compression. As discussed in the section of RF systems, the harmonic number of 3.5 is chosen for effective bunch lengthening. The half-integer gives an opportunity to simultaneously store short and long bunches bucket by bucket. This scheme for storing the short bunches will not require any additional installation of hardware. The shortest bunch length achieved by the 3.5th harmonic system is several picosecond longer than that by the mm-iFEL scheme, but it may still be useful for some experiments.

In the case of bunch slicing, a laser slicing technique [32] is as well one of the candidates for our purpose. The biggest advantage is the synchronization with a pump laser below a picosecond, since the X-ray pulse is sliced by the laser itself. The electron energy of 6 GeV requires a big laser with the peak power of Tera-watt region, but it is already available in a market. The peak brilliance tends to be lower compared with other schemes that compress bunches instead of slicing bunches. It is necessary to investigate whether the slicing technique is suitable for the SPring-8 II user experiments as well as is feasible at the site.

The main features of the three schemes mentioned above are summarized in Table 5.7. More detailed discussion is found in Ref. [1].

Table 5.7: Comparisons of pulse length, repetition rate and peak brilliance of three possible schemes. Peak brilliances are values relative to that from an ultra low emittance bunch of 35 pm·rad which is stretched to 40 ps (r.m.s.).

	pulse length (r.m.s.)	repetition rate	relative peak brilliance
mm-wave iFEL	$\sim$ 0.6 ps	$>$ 208 kHz	2 $\sim$ 5
3.5th harmonic RF	3 $\sim$ 4 ps	$>$ 208 kHz	4 $\sim$ 5
laser slicing	$<$ 1 ps	$\sim$ 1 kHz	$<$ 0.1

5.4 Design Alternatives

The baseline design has been presented in this chapter. The new lattice features 6 bend achromat with damping wigglers at the electron energy of 6 GeV. The stored current is assumed to be 300 mA at maximum based on the heat load estimation. In order to achieve the extremely small emittance under constraints such that the ring circumference is the same as the current one, we do not necessarily rely on existing technologies; instead, we take into consideration extensive technology developments in almost every key component so that we try to push the limit of the storage ring as further as possible.

Through the overall study via design iteration between lattice and hardwares, we have addressed technical challenges that are critical to our goal. The major challenges are listed below;

- Strong multipole magnets
- Alignment precision of magnets and new commissioning strategy for sending electron beams at the center of magnets
- Vacuum chambers equipped with radiation slots that accommodate strong magnets with small bore radii
- New injection scheme based on a fast kicker
- New RF systems including superconducting higher harmonic apparatus

The parameters presented in the report may change in detail as the design study is further proceeded. For example, the stored current could be decreased if lower emittance, i.e., smaller IBS effect, with smaller current would be preferred by users. Collective effects may also limit an acceptable maximum current when it is thoroughly studied. The RF frequency might be changed as well. The current setting, 508.58 MHz, is based on a cost effectiveness, because it allows us to continue using the existing RF systems. Another frequency, e.g., 476 MHz, might be picked up if the harmonic relation between the new storage ring and the XFEL linac, which runs at 2,856 MHz and its sub/higher harmonics, should be taken. The detailed parameters will be determined from perspectives of both accelerator and experiment sides. In addition, some of *major* parameters might be modified, if necessary. We shall here briefly overview design alternatives that may be eventually necessary to overcome the above challenging issues.

One of the possibilities is to change an electron energy. So far we have chosen 6 GeV to reduce the natural emittance. More precisely, the emittance including the IBS effect starts to increase below the electron energy of 4 to 6 GeV for a bunch current of 0.1 to 1 mA. Since the SPring-8 II aims to cover the spectral range of up to 100 keV as the current SPring-8 does, the electron energy of 6 GeV is chosen. As indicated in Section 5.2, the decrease of the electron energy relies on recent and future advances in insertion devices. Depending on demands from

Table 5.8: Comparison of power consumption (rough estimation). For SPring-8, the power consumption by the linac and the booster ring are included, while the new design does not because the two injectors will not be used. Accelerator voltages of 16, 12, and 4 MV are respectively assumed for SPring-8, new design, and the alternative. Power consumption for the higher harmonic system is assumed to be 0.4 MW for the new design and the alternative.

	Energy[GeV]/Current[mA]	Magnets [MW]	RF system [MW]	Total [MW]
SPring-8	8.0 / 100	4.1	7.7	11.8
New design	6.0 / 300	2.0	5.9	7.9
Alternative	4.5 / 300	1.5	1.9	3.4

future experiments, it may be required to increase the energy back to higher value to push the spectral range into even harder X-rays. So far, we have not found a strong reason to go beyond 8 GeV, though. Another candidate is to decrease the energy at the expense of especially flux at high photon energies above 100 keV. First, the lower energy effectively serves experiments at soft X-rays to X-rays of about tens of keV. The motivation from the accelerator point of view is that the lower energy helps relax some of accelerator parameters, including the above major challenging issues; the required magnetic field of magnets and kicker field of the injector are proportional to the electron energy, and the RF system could be smaller. The requirement for damping wigglers and the related apparatus such as absorbers would be also relaxed. Since the electron emittance is proportional to the square of the electron energy, the coherent fraction is also improved by decreasing the electron energy. Moreover, the electron energy of lower than about 5 GeV starts to bring the Touschek lifetime to a new regime where the Touschek lifetime is expected to quickly increase as the emittance becomes small [33].

Another concern is a power consumption. The expected power consumptions of current and planned accelerator complex are compared in Table.5.8. Here, accelerator voltages of 16, 12, and 5 MV are respectively assumed for the current SPring-8, the new design, and the alternative, for the similar over-voltage factor. See the figure caption for other assumptions. One can see that the energy consumption is suppressed at 6 GeV even with the average current of 300 mA. It should be emphasized, therefore, that the newly designed ring already indicates the energy efficiency. Since the new ring is expected to yield higher brilliance than the current one by two to three of orders of magnitude (see Chapter 6 in detail), it follows that the energy efficiency would be significantly improved. The possibility of decreasing the electron energy below 6 GeV should even assist it as is shown in Table.5.8. The power consumption for the 4.5 GeV/300 mA ring would be less than half of the current one. At present the energy of 6 GeV is the best compromise for our purpose, which may be adjusted more at later stages.

Another important design alternative is related to a combined function magnet, especially that combines dipole and quadrupole fields. The combined function magnets have been employed at MAX-lab [34], especially for the MAX-IV storage ring, for example. Such a magnet can decrease the packing factor, therefore a lattice with bending magnets combined with quadrupoles has been as well designed. The known challenging issue with the combined magnet is an alignment error. The dipole magnets should be carefully aligned in order to avoid undesirable kick of an orbit by quadrupole fields [1]. Another type of combined function magnet, such as sextupole magnets coupled with quadrupole fields, are also being considered.

References

[1] The SPring-8 Upgrade Plan Working Group, *Preliminary Accelerator Design of SPring-8 II*, to be published.

[2] T. Watanabe *et al.*, Proc. of IPAC'11 (Sep. 4–9, 2011), San Sebastián, Spain (2011).

[3] A. Ropert, *et al.*, Proc. of EPAC'00, Vienna, Austria, p. 83 (2000).

[4] H. Wiedemann, *Particle Accelerator Physics*, Third Edition, Springer (2007).

[5] S.Y. Lee, *Accelerator Physics*, World Scientific (1999).

[6] D. Einfeld *et al.*, Proc. of EPAC'96, Sitges, Spain, p. 638 (1996); D. Einfeld and M. Plesko, Nucl. Instrum. Meth. A **335**, 402 (1993).

[7] L. Emery and M. Borland, Proc. of PAC'03, Portland, Oregon, USA, p. 256 (2003).

[8] M. Borland, Nucl. Instrum. Meth. A **557**, 230 (2006).

[9] K. Tsumaki and N. Kumagai, Nucl. Instrum. Meth. A **565** , 394 (2006); K. Tsumaki and N. Kumagai, Proc. of EPAC'06, Edinburgh, UK, p. 3362 (2006).

[10] S.C. Leemann *et al.*, Phys. Rev. ST-AB **12**, 120701 (2009).

[11] R. Hettel *et al.*, Proc. of EPAC'08, Genoa, Italy, p. 2031 (2008); *PEP-X Status Report* (2008); K. Bane *et al.*, *A Design Report of the Baseline for PEP-X: an Ultra-Low Emittance Storage Ring*, SLAC-PUB-13999 (2010).

[12] Y. Shimosaki, "*Nonlinear Resonance Analysis for Correction of Off-Momentum Dynamic Aperture*", 2nd Workshop on Nonlinear Beam Dynamics in Storage Rings (Nov. 2–4, 2009), DIAMOND, United Kingdom (2009).

[13] K. Soutome *et al.*, Proc. of IPAC'10, Kyoto, Japan, p. 2555 (2010).

[14] Y. Shimosaki *et al.*, "*Lattice Design of a Very Low-emittance Storage Ring for SPring-8-II*", Proc. of IPAC'11 (Sep. 4-9, 2011), San Sebastián, Spain (2011).

[15] Y. Shimosaki and K. Takayama, Phys. Rev. E **62**, 2797 (2000).

[16] H. Tanaka *et al.*, Nucl. Instrum. Meth. A **431**, 396 (1999); Erratum, *op. cit.*, A **440**, 259 (2000).

[17] M. Takao, Phys. Rev. E **72**, 046502 (2005); M. Takao *et al.*, Phys. Rev. E **70**, 016501 (2004).

[18] K. L. Brown, IEEE Trans. Nucl. Sci. **NS-26**, 3490 (1979).

[19] L. Emery, Proc. of PAC'89, Chicago, USA, p. 1225 (1989).

[20] K. Oide and H. Koiso, Phys. Rev. E **47**, 2010 (1993).

[21] T. Harada, Y. Kobayashi, T. Miyajima and S. Nagahashi, Phys. Rev. ST-AB **10**, 123501 (2007).

[22] T. Naito *et al.*, Proc. of PAC'09, Vancouver, BC, Canada, p. 1620 (2009).

[23] M. Borland *et al.*, AIP Conf. Proc. **1234**, 501 (2010).

[24] Y. Kawashima, H. Ego, Y. Ohashi, and M. Hara, Proc. EPAC'08, Genoa, Italy, p. 1485 (2008).

[25] H. Ego *et al.*, Nucl. Instrum. Meth. A **400**, 195 (1997).

[26] M. Borland, "*elegant: A Flexible SDDS-Compliant Code for Accelerator Simulation*", Advanced Photon Source LS-287 (2000).

[27] P. Marchand, Proc. of the 18th Particle Accelerator Conference, New York, USA, p. 989 (1999).

[28] A. Hofmann and S. Myers, CERN ISR-TH-RF/80-26 (1980).

[29] A. Temnykh, Proc. of PAC'97, p. 3218 (1997).

[30] Y. Kawashima, T. Asaka, and T. Takashima, Phys. Rev. ST-AB **4**, 082001 (2001).

[31] V. N. Litvinenko, "*Femtosecond e-beams in storage rings*", Femtosecond Beam Science edited by M. Uesaka, Imperial College Press, p. 80 (2005).

[32] R. W. Schoenlein *et al.*, Appl. Phys. B **71**, 1 (2000).

[33] V. N. Litvinenko, ICFA Workshop (1999).

[34] http://www.maxlab.lu.se/